FLEXURAL PERFORMANCE OF FRP-REINFORCED MASONRY WALLS

Navid Sasanian[1] and Khaled Galal[2]

[1] M.A.Sc. Graduate Student, Department of Building, Civil and Environmental Engineering, Concordia University, Montréal, Québec, Canada H3G 1M8

[2] Associate Professor, Department of Building, Civil and Environmental Engineering, Concordia University, Montréal, Québec, Canada H3G 1M8

ABSTRACT

The objective of this paper is to assess the out-of-plane flexural performance of masonry walls that are reinforced with Glass Fibre-Reinforced Polymers (GFRP) rods, as an alternative for steel rebars. Eight 1mx3m full-scale walls were constructed using hollow concrete masonry unit and tested in four-point bending with an effective span of 2.4 m between the supports. The walls were tested when subjected to increasing monotonic loads up to failure. The applied loads would represent out-of-plane loads arising from wind, soil pressure, or earthquake. One wall is unreinforced; another wall is reinforced with customary steel rebars and the other six walls are reinforced with different amounts of GFRP reinforcement. Two of the GFRP-reinforced walls were grouted only in the cells were the rods were placed in order to investigate the effect of grouting the empty cells. The force-deformation relationship of the walls and the associated strains in the reinforcement were monitored throughout the tests. The relative performances of tested walls are assessed in order to quantify the effect of different design variables. The range of GFRP reinforcement ratios covered in the experiments was used to propose a capacity diagram for design of FRP-reinforced masonry walls similar to that of reinforced concrete elements.

KEYWORDS: FRP reinforcement, reinforced masonry, walls, flexure.

INTRODUCTION

Masonry walls are considered as one of the most common structural masonry elements that are broadly employed to undertake axial and lateral loads. Depending on the application and also the orientation of masonry walls, these elements can be submitted to out-of-plane bending actions arising from wind, soil pressure, or seismic excitations, in which situations, the role of flexural reinforcement is critically influential in flexural strength, behaviour, and serviceability of the walls.

Fibre-Reinforced Polymers (FRP) have been studied and used extensively to reinforce concrete structures as a new substitute for steel reinforcement over the past ten years [1]. FRP bars have been proven to be an effective means to replace steel reinforcement in various concrete structures such as bridge decks and parking garages. In addition to their superior durability, mainly due to

outstanding non-corrosive characteristics, these composite materials have the benefits of high strength-to-weight ratio, considerable fatigue properties, and electromagnetic transparency. Moreover, their usage in concrete structures has been codified in Canadian Highway Bridge Design Code (CHBDC) [2]. Lower fire resistance and higher costs are considered as the disadvantages therein. However, the former is not an issue in the case of concrete masonry in that the minimum required cover, which is found to be 64mm or less [1], is fulfilled by the dimensions of masonry units. Moreover, the decreasing cost of FRP as well as lower transportation and handling costs of lighter materials are making the use of FRP in construction more competitive. Significant amount of work has been directed to utilizing different types of FRP that are externally bonded or mounted on the surface of masonry walls for strengthening reinforced and unreinforced masonry (URM) walls [3-7]. There are also a few experimental research works that exploited FRP for externally reinforcing URM walls [8-10]. On the contrary, to the authors' knowledge there has been no effort corresponding to the use of FRP as interior reinforcement of masonry structural elements. In a study conducted by Mierzejewski *et al.* [10], near surface mounted GFRP rods were used to reinforce URM walls for out-of-plane flexure. Although external reinforcement provided the advantage of spreading the reinforcement away from neutral axis, debonding of the GFRP rods, which was observed as the mode of failure of some of the tested walls, underscores the effectiveness of internal reinforcement.

This paper presents the test results of an experimental and analytical study. The experimental phase includes testing supplementary masonry prisms as well as eight full-scale masonry walls, six of which were reinforced with GFRP rods. All the auxiliary specimens (masonry prisms) and full-scale walls were constructed by domestic registered masons representing the current method of practice in Québec during four consecutive days. The GFRP rebars used in this study are known as V-ROD^{TM} and manufactured by Pultrall Inc. located in Québec. As the major parameters of the study, different amounts of GFRP reinforcement and the extent of grout-filling are taken into account. Moreover, an analogous steel-reinforced masonry wall, from the design point of view, is tested and compared with two of the GFRP-reinforced walls. Furthermore, a capacity diagram is proposed based on the performance of the tested walls for designing GFRP-reinforced masonry elements in flexure.

AUXILIARY LABORATORY TESTS FOR THE MASONRY ASSEMBLAGE

In order to determine the compressive strength of the masonry assemblage a series of five unreinforced grouted prisms, five-block high and one-block wide, were tested as stated in ASTM C1314-02a [11]. The average compressive strength (f'_m) was determined to be 10.9 MPa with a coefficient of variation of 6.4% neglecting the result of the second prism. Typical splitting of the concrete blocks was observed as the dominant mode of failure initiated by cone shape shear cracks. For the purpose of estimating the cracking moment of the walls, another series of five prisms were tested in a four point bending setup described in ASTM E518-02 [12]. Prisms with the height of seven blocks and width of one block were tested such as to locate the two point loads and supports in the middle of the block and also to provide for sufficient span-to-depth ratio [12]. The average flexural bond strength of the prisms, also referred to as modulus of rupture (R), was reported 1.11 MPa with a coefficient of variation of 9.5% disregarding the result of the last prism.

TEST ON FULL-SCALE MASONRY WALLS

The main part of the experimental program consists of testing eight full scale walls under out-of-plane bending. Each specimen is a single-wythe masonry wall with nominal dimensions of 1mx3m that is made of 15 courses of two and a half concrete blocks with half running bond. As can be seen in table 1, the first wall is unreinforced, the second wall is reinforced with customary steel rebars, and the other six walls are reinforced with different GFRP reinforcement ratios. Wall number 6 and 8 are identical, with regard to the reinforcement ratio, to wall number 5 and 7, respectively; yet they are only grouted at the locations of the longitudinal reinforcements, to study the effect of not grouting the empty cells. Bed joint reinforcement that consisted of truss type 3.2mm (⅛″) gauge wire was placed in every other joint (with a spacing of 400mm). The wall designation refers to: 1) type of reinforcement (Steel, GFRP, or Unreinforced), 2) number and size of the rebars, and 3) the extent of grouting (Full or Partial). Walls were constructed, cured, and hardened vertically. Afterwards, they were transferred and laid horizontally on the setup using a steel braced frame designed for this purpose. Three of the GFRP-reinforced walls were gradually unloaded and reloaded after the failure to determine the permanent (inelastic) displacement and the post-failure strength; but for other walls it was not safe and secure to do so.

Table 1: Matrix of the full-scale masonry walls

Wall	Reinf. material	Average effective depth (mm)		Reinf. ratio (%)		Extent of grouting
		Nominal	Measured	Nominal	Measured	
U-F	—	—	—	—	—	Fully
S-5M10-F	Steel	95	90	0.53	0.56	Fully
G-3#10-F	GFRP	95	95	0.25	0.25	Fully
G-3#13-F	GFRP	95	100	0.42	0.40	Fully
G-3#13-P	GFRP	95	105	0.50	0.45	Partially
G-4#13-F	GFRP	95	105	0.56	0.51	Fully
G-4#13-P	GFRP	95	125	0.61	0.46	Partially
G-3#19-F	GFRP	95	125	0.89	0.69	Fully

TEST SETUP AND INSTRUMENTATIONS

The masonry walls were tested in a third-point loading setup, shown schematically in Figure 1, with an effective span of 2.4 m. Two point loads, at third spans, were applied and monotonically increased by a 15-ton hydraulic actuator, reacting against a steel loading frame, up to the ultimate failure. Load was transferred through the loading apparatus and applied over two 152.4mm (6″) wide channels to avoid crushing the blocks due to stress concentration. The walls were tested while positioned horizontally on a hinge at one end and a roller at the other end, similar to previous tests on masonry walls performed by several researchers. At ten different points of each tested wall, potentiometers were located to read the displacement (three at mid-span, six at third-spans and one at quarter-span), such that to have the longitudinal profile of the wall at each stage and also to make sure that the wall is not tilted or twisted in width due to probable test setup imperfections. The maximum axial strain, assumingly in the mid-span, for every reinforcing rod (GFRP and steel) was recorded using strain gauges that had been installed on the rods before construction. Furthermore, the strain in two of the reinforcing rods for each reinforced wall at quarter-span was recorded.

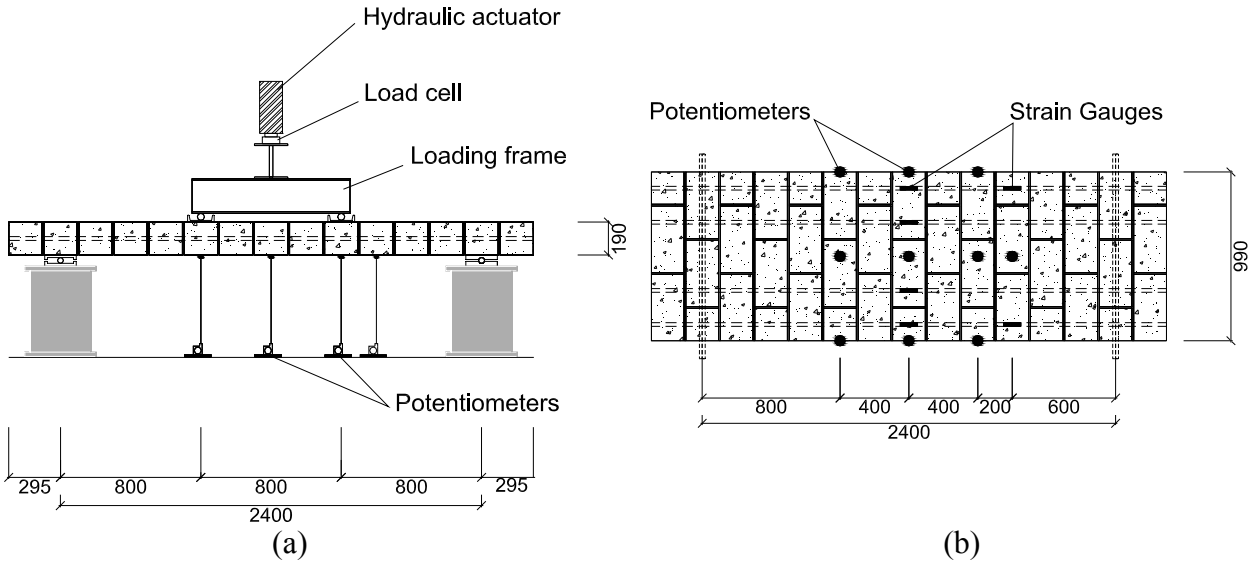

Figure 1: Test setup and instrumentations: (a) elevation of the test setup for the full-scale walls; (b) plan and instrumentation for a typical wall reinforced with four rebars

CRACKS AND DEFORMATION

Based on flexural bond strength of the tested auxiliary prisms, no cracking was expected to occur due to the self weight of the walls. The first crack was generated in the constant moment zone as the applied moment reached the vicinity of the expected cracking moment. More flexural cracks as well as shear cracks outside the constant moment zone started to appear by increasing the applied moment which also deepened and widened the existing cracks gradually. All the cracks were initiated primarily from the bottom of the section at the interface of masonry unit and mortar and developed upward in the grout. Each crack resulted in separating the block from mortar along the lower face shell at one instant and as a result the deflections increased dramatically. The threshold of flexural strength was preceded by enormous opening in one of the block-mortar joints between the two point loads and cracks in the concrete blocks that culminated in crushing of the masonry units in compression. In some of the tests, the mortar in the failed bed joint spalled off the compression side. The unreinforced wall experienced a sudden failure that followed a crack formed in one of the joints in the constant moment region. For the steel-reinforced wall, the shear cracks appeared, after the rebars had yielded, in two bed joints which underwent the maximum shear force. Another finding was the effect that the extent of grouting had on the cracking load. The partially grouted walls cracked at fairly lower levels of applied load when compared to their analogous companions. However, it can be stated that type of the reinforcement had not a significant effect on the onset of cracking, nor did it on the immediate width of the cracks.

LOAD-DEFLECTION AND LOAD-STRAIN CURVES

In order to take into consideration the self weight of the walls, the equivalent load that produces the same moment as the distributed self weight over the wall does was added to the recorded applied load. This was done without missing any useful information meaning that, as mentioned

before, the expected cracking moment (6.6 kN.m) was larger than the moment produced by the own weight of the walls (between 2.5 and 4.1 kN.m). Furthermore, a pair of temporary supports were fabricated to carry the weight of the walls and removed after having launched the data acquisition system, so that the deflections due to the self weight of the walls would not be missed either. Having the equivalent dead load and its corresponding deflection and strain, the initial portion of the force-deformation and force-strain curves was superimposed to that of live load. The drastic drops in the recorded loads are in agreement with the cracks' occurrence, while the tiny drops can be associated with the existing cracks widening or extending in depth which also happened intermittently. It is observed that after each drop the load has caught up to a higher level but with a diminished stiffness. It illustrates how the section approaches to the cracked section properties progressively. Figure 2 (a) shows the load versus the deflection at mid-span of the tested walls. The remarkably poor strength and deformation of the wall U-F simply depicts the drastic effect that the use of even smallest amount of GFRP reinforcement can have on the flexural performance of the masonry walls. More importantly, the sudden failure is replaced with ample deformation of the walls after the first crack followed by ultimate failure. Another notable observation is that G-3#19-F with the largest reinforcement ratio, when compared to S-5M10-F, shows that we can reach higher capacities with acceptable deformability that could not be achieved by steel-reinforced masonry walls due to the constraint of not exceeding the balanced reinforcement ratio. As one of the authors' intentions, the relative performance of the steel-reinforced wall is also demonstrated and compared with that of the walls G-4#13-F and G-4#13-P which were designed to reach the same ultimate limit flexural capacity. Looking at the same graph, it can be concluded that grout-filling the empty cells does not have a positive effect on the general performance of the walls. Wall G-4#13-P exhibited significantly higher strength compared to wall G-4#13-F; this could be attributed to the actual location of the GFRP rods inside the cells which was determined for the walls after the tests. The average effective depth of the bars for wall G-4#13-P was found to be 125mm, while for wall G-4#13-F it was 105mm.

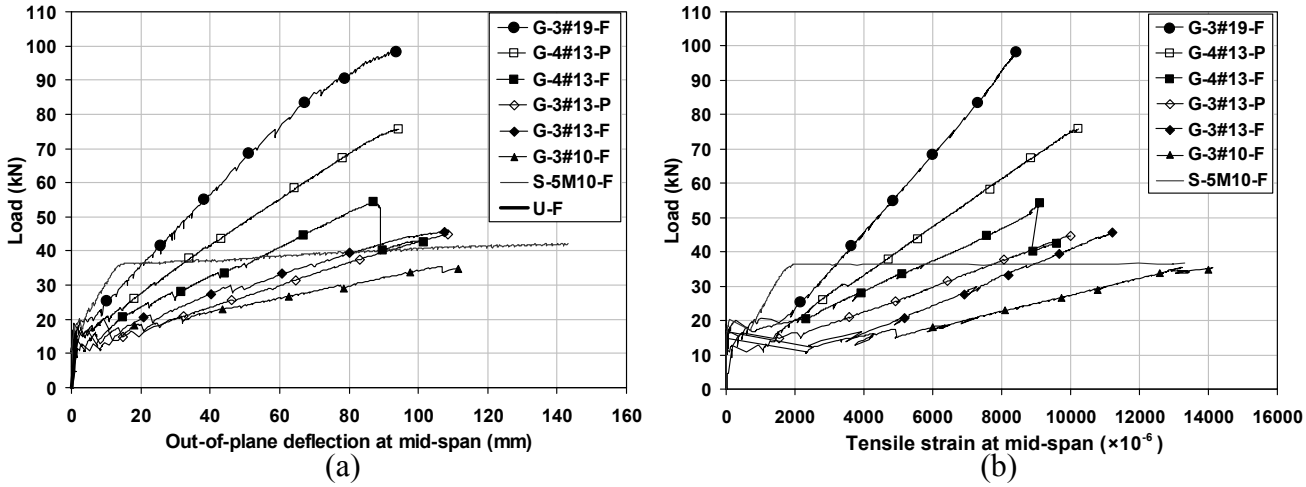

Figure 2: Behaviour of the tested walls: (a) Load-deflection performance of the walls; (b) load-strain performance of the walls

Figure 2 (b) illustrates the change in tensile strains of the longitudinal reinforcements with applied lateral load. Since the reinforcing rods are in the vicinity of the neutral axis of the gross section, the strain and accordingly stress in the FRP are negligible prior to cracking. However,

the curves show that the tensile strain and accordingly stress increase linearly with the applied load up to the failure of the walls.

MODE OF FAILURE AND POST FAILURE BEHAVIOUR

The unreinforced wall encountered a sudden failure right after the first flexural crack formed. For the reinforced walls, the failure was always in compression zone of the masonry compound even though it was preceded by different phenomena (see Figure 3).

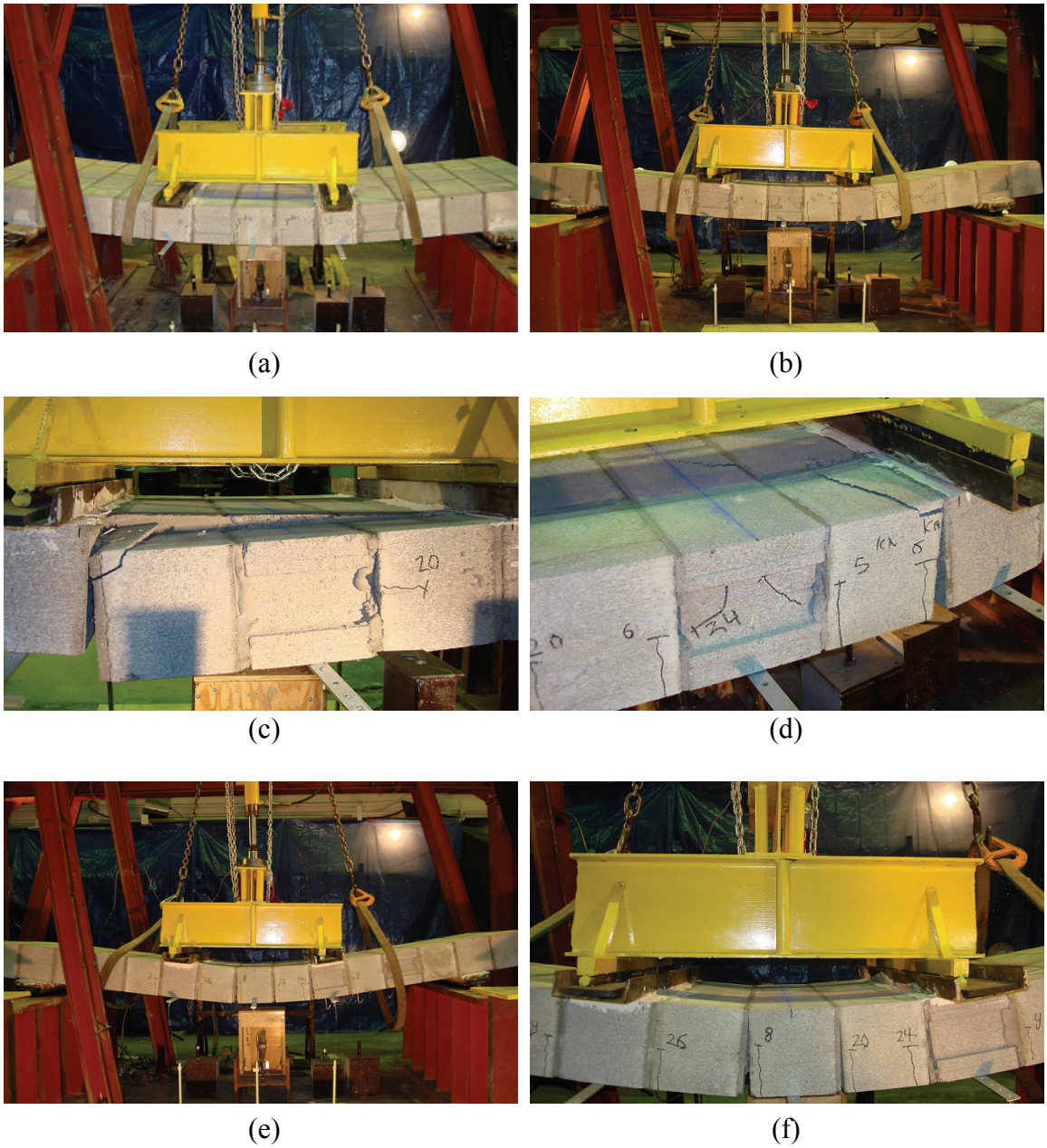

(a) (b) (c) (d) (e) (f)

Figure 3: Failure of the walls: (a) Flexural cracks at the joints in constant moment zone; (b) deformed shape of a GFRP-reinforced wall close to failure; (c) a strip of grouted blocks separated from wall G-3#13-P; (d) a wide diagonal crack developed on the compression side of wall G-3#13-F; (e) deformed shape of the steel-reinforced wall close to failure; (f) shear cracks did not appear for the steel-reinforced wall

G-3#10-F failed after the joint next to the point load inside the moment zone had opened up significantly and the top face shell of one cell next to the same bed joint was crushed. Same thing happened for G-3#13-F, G-4#13-F, G-4#13-P, and G-3#19-F; however, there were some diagonal cracks detected on the side of the blocks next to the failed joints (Figure 3 (b)). G-3#13-P failed after a strip of 3 consecutive cells separated on one side of the wall inside the constant moment zone (Figure 3 (c)). A half block on one side was separated and misaligned before the failure of G-4#13-F. For the case of G-3#19-F, the cracks in the masonry units were relatively wide. G-3#13-F, G-4#13-P, and G-3#19-F experienced shear cracks on the side of masonry units outside the constant moment region. For G-3#13-F, these cracks joined a mortar-block interface next to the point load which widened considerably, nevertheless the failure was induced by a long and wide crack on the upper side of the wall that was diagonally developed over the constant moment zone (Figure 3 (d)). The steel-reinforced wall simply failed after the joint cracks were widened and compressive cracks had appeared on the compression side of the blocks, although no shear crack was detected on the masonry units (Figure 3 (e) and (f)).

G-3#13-F, G-3#13-P, and G-3#19-F were unloaded reloaded after the failure in order to investigate their post-failure strength and inelastic deformation. Their inelastic deformations as percentages of their total deformations were found to be 7.8%, 39%, and 36.5%, respectively. The post-failure resistances corresponding to these walls found to be 34.4%, 46.6%, and 47.3% of the ultimate flexural capacity, respectively. The notable observation therein is that not only did the post-failure strength of the FRP-reinforced walls exceed their dead loads, but also it helped to encounter considerable amount of applied live load.

SECTION ANALYSIS IN FLEXURE

The tested walls' section analysis is done using the common method of ultimate strength conditions that is adopted in CSA S304.1 [13]. For the case of GFRP-reinforced sections, necessary modifications are adopted to the procedures in accordance with ISIS M03-01 [14]. The approach employed in this part is assumed to be appropriate, in that all the tested walls failed due to the compressive failure of the masonry. The analysis is carried out assuming that 1) plane sections remain plane, 2) the strain varies linearly in the depth of the section, 3) deformations are small, 4) tensile strength in the masonry and compressive strength of composites are negligible, 5) the GFRP rods bond with concrete with no interfacial slippage, 6) the ultimate compressive strain of the masonry compound is 0.003 as suggested in CSA S304.1 [13], and 7) all the GFRP-reinforced sections fail due to masonry crushing as they were designed to be over reinforced. As for the GFRP rods, the stress-strain relationship is presumed to be linear elastic up to the point where the rupture happens. Although the rods were initially intended to be placed in the middle of the unit cells with an effective depth (d) of 95mm, after the failure of each wall, the actual d of was measured at the failed section to be used in the analyses. This value ranged for the walls from 100mm to 125mm.

The outcomes of the numerical evaluations state that the theoretical prediction is fairly conservative, since the ratio of experimental to theoretical ultimate strength varies from 1.13 to 1.28. In order to have a more accurate prediction, in lieu of equivalent Whitney stress block, three different stress-strain models that account for more realistic stress-strain behaviour of concrete masonry were adopted in the aforesaid procedure. Dhanasekar and Shrive [15] have proposed two stress-strain curves, one simple and one refined. Furthermore, Priestley and Elder

[16] suggested the use of another model for concrete masonry. All the three curves were integrated into the walls' section analysis leading to closer estimate of strengths, even though still slightly conservative. The one most conforming with the results of the tests was found to be the refined equation proposed by Dhanasekar and shrive [15] as brought in equation (1):

$$\sigma_m = f'_m \left(\frac{\left(1+u_0\left(1+u_1\right)\right)x}{u_0\left(1+u_1 x\right)+x^{1+u_0}} \right) \quad (1)$$

Where u_0 and u_1 are constants taken as 1.5 and 1.0 respectively for grouted concrete masonry and 2.1 and 0.1 for ungrouted concrete masonry, and x is the ratio of strain to the strain at maximum stress. The ratio of experimental to theoretical ultimate strength using the selected stress-strain curve ranges from 1.01 to 1.15. The results of section analysis and wall tests are compared and tabulated as well as the maximum lateral deflections and tensile strains, cracking moments, and modes of failure of the walls in table 2.

Table 2: Summary of the test results for the full-scale walls

Wall	$M_{n\,(exper.)}$ (kN.m)	$M_{n\,(analyt.)}$ (kN.m)	$\frac{M_n\ (exper.)}{M_n\ (analyt.)}$	Max. Deflection (mm)	Max. tensile strain ($\times 10^{-6}$)	Mode of failure
U-F	5.6	6.4	0.87	1.4	—	Tensile in bed joint
S-5M10-F	16.9	16.2	1.05	143.2	—	↑
G-3#10-F	14.2	13.1	1.09	111.4	14002	↑
G-3#13-F	18.3	17.7	1.03	107.4	11218	Compressive in masonry
G-3#13-P	17.9	17.6	1.02	108.5	9997	Compressive in masonry
G-4#13-F	21.7	21.4	1.01	108.9	9613	Compressive in masonry
G-4#13-P	30.3	27.3	1.11	94.3	10235	↓
G-3#19-F	39.3	34.2	1.15	93.6	8440	↓

DESIGN DIAGRAM

The main objective of this study was to develop a facilitated approach to design the masonry walls for out-of plane bending when reinforced with GFRP rebars. For designing FRP-reinforced concrete (FRP-RC) members in flexure, design charts are provided by ISIS M03 [14] for a given cross-sectional dimensions. The reinforcement ratio required for a certain amount of resistant moment can be chosen simply by following the proper curves of the charts. Having the results of the tested walls for different reinforcement ratios, it is tried to propose the design diagram illustrated in Figure 4. The theoretical predictions are based on f'_m equal to 10.9 MPa and corresponding properties for different diameters of GFRP rods. However, in order to simplify the use of this type of diagrams, they can be achieved eventually based on the average properties of the composites. The results of the tested walls seem to have consistency with the predicted values, that is to say the methods of analysis presented herein can be relied on to design this type of structural members.

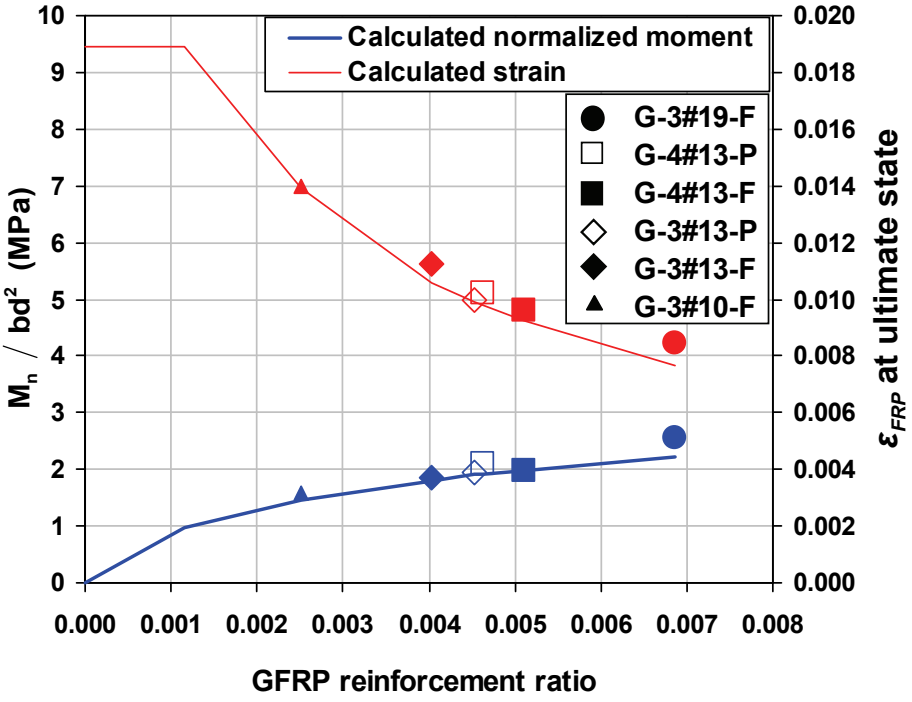

Figure 4: Proposed capacity chart for designing masonry walls reinforced with GFRP rods

CONCLUSIONS

Eight full-scale masonry walls (unreinforced and reinforced with steel and GFRP rebars) were built and tested under out-of-plane bending condition. The behaviour of the walls was surveyed by monitoring the crack patterns and measuring the mid-span deflections and tensile strains of the reinforcing rebars up to the ultimate failure.

All the GFRP-reinforced walls encountered flexural failure due to the compressive failure of masonry as opposed to the unreinforced wall that collapsed due to tensile failure in the bed joint. The two GFRP-reinforced specimens that were comparable to the steel-reinforced wall reached relatively higher strengths. Although the steel-reinforced one experienced more deformation, the GFRP-reinforced walls had adequate deformability to forewarn the failure. The performance of G-3#19-F compared to that of S-5M10-F showed that we can reach higher capacities with acceptable deformability that could not be achieved by steel-reinforced masonry walls. Except for G-3#19-F, the depth of the compressive zone was found to be less than the face shell thickness. Hence, grouting the cells with no reinforcement is not necessarily effective since the grout is not contributing to the bending actions of the section. The results of the wall tests acknowledged this matter.

The observations and findings of this research yield to a better perceptive of masonry walls' inelastic behaviour in out-of-plane bending when reinforced with GFRP rods that can assist in theorizing a limit-states design methodology in future code for masonry structures reinforced with FRP; however, the authors believe that further studies and experiments on FRP-reinforced masonry are required in order to validate and generalize the outcomes of this experimental program.

ACKNOWLEDGEMENTS

The authors wish to acknowledge the financial supports of Natural Sciences and Engineering Research council of Canada (NSERC), le Fonds Québécois de la Recherche sur la Nature et les Technologies (FQRNT), and Centre d' Études Interuniversitaire sur les Structures sous Charges Extrêmes (CEISCE). l'Association des Entrepreneurs en Maçonnerie du Québec (AEMQ), Canada Masonry Design Centre (CMDC), and Tomassini et frères Ltée who assisted us extensively through the team research project are gratefully appreciated.

REFERENCES

1. Saafi, M. (2002). "Effect of fire on FRP reinforced concrete members." Composite Structures, 58, 11–20.
2. Canadian Standards Association (CSA). (2006). "S6-06: Canadian Highway Bridge Design Code (CHBDC)." Toronto, Ontario.
3. Kiss, R. M., Kollar, L. P., Jai, J., and Krawinkler, H. (2002). "FRP strengthened masonry beams, part 2: test results and model predictions." Journal of Composite Materials, 36(9), 1049-1063.
4. Ghobarah, A., and Galal, K. E. (2004). "Out-of-plane strengthening of URM walls with openings" ASCE Journal of Composites for Construction, 8(4), 298–305.
5. Tan, K. H. F., and Patoary, M. K. H. (2004). "Strengthening of masonry walls against out-of-plane loads using fiber-reinforced polymer reinforcement." ASCE Journal of Composites for Construction, 8(1), 79–87.
6. Galati, N., Tumialan, G., and Nanni, A. (2006). "Strengthening with FRP bars of URM walls subject to out-of-plane loads." Construction and Building Materials, 20(1-2), 101-110.
7. Turco, V., Secondin, S., Morbin, A., Valluzzi, M. R., and Modena, C. (2006). "Flexural and shear strengthening of un-reinforced masonry with FRP bars. "Composites Science and Technology, 66, 289–296.
8. Gilstrap, J. M., and Dolan, C. W. (1998). "Out-of-plane bending of FRP reinforced masonry walls." Composites Science and Technology, 58, 1277–1284.
9. Hamoush, S. A., McGinley, M. W., Mlakar, P., and Terro, M. J. (2002). "Out-of-plane behaviour of surface-reinforced masonry walls." Construction and Building Materials, 16(6), 341–351.
10. Mierzejewski, W., Fam, A., MacDougall, C., and Chidiac, S.E. (2008). "Out-of-Plane Testing of Masonry Walls with Near-Surface Mounted (NSM) Reinforcement." 2nd Canadian Conference on Effective Design of Structures, McMaster University, Hamilton, Ontario.
11. American Society of Testing and Materials (ASTM). (2002). "C1314-02: Standard Test Method for Compressive Strength of Masonry Prisms." West Conshohocken, Pa.
12. American Society of Testing and Materials (ASTM). (2002). "C518-02: Standard Test Method for Flexural Bond Strength of Masonry." West Conshohocken, Pa.
13. Canadian Standards Association (CSA). (2004). "S304.1-04: Design of Masonry Structures." Mississauga, Ontario.
14. The Canadian Network of Centres of Excellence on Intelligent Sensing for Innovative Structures (ISIS Canada). (2001). "Design manual No. 3: Reinforcing concrete structures with fibre reinforced polymers." Winnipeg, Manitoba, Canada.
15. Dhanasekar, M., and Shrive, N. G. (2002). "Strength and Deformation of Confined and Unconfined Grouted Concrete Masonry." ACI Structural Journal, 99(6), 819-826.
16. Priestley, M. J. N., and Elder, D. M. (1983). "Stress-strain curves for unconfined and confined concrete masonry." ACI Journal, 80(3), 192–201.
17. Drysdale, R.G. and Hamid, A.A. (2005). "Masonry structures – Behaviour and design." Canada Masonry Design Centre, Mississauga, Canada.
18. Masonry Standards Joint Committee (MSJT). (2005). "Building Code Requirements for Masonry Structures." ACI 530/ASCE 5/TMS 402-99, the Masonry Society, Boulder, Co.